JOURNAL OF MATERIALS SCIENCE **39** (2004) 5735–5742

# Synthesis and characterization of TiC-reinforced iron-based composites

## Part I *On synthesis and microstructural characterization*

T. K. BANDYOPADHYAY, S. CHATTERJEE*, K. DAS
*Department of Metallurgical and Materials Engineering, Indian Institute of Technology, Kharagpur 721 302, India*
*E-mail: karabi@metal.iitkgp.ernet.in*

The present investigation establishes a liquid processing route where thermit based reactions have been used to synthesize *in-situ* TiC-reinforced Fe-based composites in a single step. The main raw material used is siliceous sand, which is a "waste" product of aluminum extraction plants. A dispersion of TiC in Fe-based matrix has been obtained by aluminothermic reduction of siliceous sand, containing oxides of different elements like iron, titanium, silicon etc., in the presence of carbon. The reduction is highly exothermic in nature and leads to a self-propagating high-temperature synthesis (SHS) of the Fe-TiC composites. The matrix structure and volume fraction of TiC of the composites have been found to depend upon the amount of carbon added in the charge. It has been found that microstructures of Fe-TiC composites are not stable at high temperature due to the nonstoichiometric nature of TiC particles. © *2004 Kluwer Academic Publishers*

## 1. Introduction

Iron matrix composites have gained attention essentially for wear resistant applications. Iron and its alloys, as engineering materials, are yet to be displaced from the top slot by polymers, ceramics, or other metals in terms of volume of consumption; thus it becomes imperative to further improve their properties. Achieving the same by ceramic particle reinforcement is possible and has been proved [1–5]. The common ceramic materials used for reinforcing Fe matrices are $Al_2O_3$, $ZrO_2$, $TiN_2$, $Si_3N_4$, TiC, $B_4C$, VC etc. Among them TiC has proved its suitability in Fe or Fe base alloys due to its high hardness, good wettability, low density, and its chemical stability with Fe-based matrices [1]. However, it is the economy of processing the composite that will decide if it is able to compete against the wide range of steels already available in the market.

Most of the work on iron-based composites has involved TiC reinforcement, which is introduced in the iron matrix through powder metallurgy route [1–4]. But the production of a composite via this route has its limitations. Mixing of matrix powder and reinforcing particle must be thorough in order to achieve uniform dispersion of the reinforcing phase. The sintering cycle and environment must be chosen critically to obtain components with near theoretical density. There is also difficulty in machining or trimming of sintered parts because of high hardness of the materials [5]. Therefore, attempts have been made to produce Fe-based composites through alternative cost effective process such as *in-situ* production of Fe-TiC composites by reaction in liquid Fe alloys [6–9]. The TiC-reinforced Fe-based composites have also been produced by direct carbothermic reduction of ilmenite ($FeTiO_3$) or rutile ($TiO_2$) in presence of Fe [10–12]. The advantage of producing Fe-based composites through carbothermic reduction of $FeTiO_3$ is the reduction of a number of steps and thereby the cost of production. The carbothermic reduction, which leads to the formation of TiC in Fe matrix, is endothermic though spontaneous above 1348.3 K [11]. Hence, the system should have enough heat to supply for the reaction besides melting the charge. In any process, energy expenditure should be minimized. An alternative energy-efficient route to produce Fe-TiC composite could be aluminothermic reduction of $Fe_2O_3$ and $TiO_2$ in the presence of C. This type of reaction involves the reduction of a metallic or a non-metallic oxide with Al to form $Al_2O_3$ and the corresponding metal or non-metal of the reactant oxide [13]. It is highly exothermic in nature and if it is initiated locally it can become self-sustaining [13]. In the present study, the aim is to produce TiC-reinforced Fe-based composites by aluminothermic reduction of siliceous sand (a waste product of the aluminum extraction industry) in the presence of carbon using a simple set-up. This sand has been used as a source of $TiO_2$ and $Fe_2O_3$. The study also includes the synthesis of composites with different matrix structures and volume fractions of TiC by varying the amount of C added in the charge, as well as by adding $TiO_2$ externally. The effect of heat

---

*R&D Section, Tata Steel, Jamshedpur 831 001, India.

0022–2461

TABLE I Chemical composition of siliceous sand

| Components | $Fe_2O_3$ | $Al_2O_3$ | $TiO_2$ | $Na_2O$ | $SiO_2$ |
|---|---|---|---|---|---|
| wt% | 73.1 | 6.26 | 8.63 | 2.51 | 3.84 |

treatment on the microstructure has been studied as well. The mechanical properties of the composites have been evaluated and described in part-II [14].

TABLE II Charge compositions for synthesis of composites

| | Masses of the reactants (in gms) | | | | |
|---|---|---|---|---|---|
| Composite | Siliceous sand | $TiO_2$ | Cast iron | Al | Graphite |
| T1 | 440 | 20 | 200 | 130 | 6 |
| T2 | 440 | 20 | 200 | 130 | 7.5 |
| T3 | 440 | 20 | 200 | 130 | 9.0 |
| T4 | 440 | 20 | 200 | 130 | 10 |
| T5 | 440 | 20 | 200 | 130 | 13 |

## 2. Experimental procedure

### 2.1. Raw material characterization

### *2.1.1. Siliceous sand*

The main raw material used is called siliceous sand. A typical sand composition is shown in Table I. The other impurities, like NiO, $Cr_2O_3$, and $V_2O_5$ make up the balance. The sand is rich in $Fe_2O_3$ and also contains a substantial amount of $TiO_2$. The $Na_2O$ may cause problem in slag-metal separation. This was taken care of by boiling sand in water. The $Na_2O$ dissolved away and the sand was ready for use after drying.

### *2.1.2. Cast iron*

White cast iron chips were used as a source of C as well as matrix Fe. The typical composition of the cast iron is 3.86% C, 1.2% Si, 0.2% Mn, 0.5% P, and balance Fe (in wt%).

### *2.1.3. Graphite powder*

Fine graphite powder of particle size around 40 $\mu$m was used as a source of C.

### *2.1.4. Aluminum (Al)*

Laboratory grade Al powder of particle size around 50 $\mu$m was used as reductant.

### *2.1.5. Titania ($TiO_2$)*

Laboratory grade fine $TiO_2$ powder was used as a source of Ti to adjust the volume fraction of TiC.

## 3. Synthesis

### 3.1. Charge preparation

The influence of amount of C in the charge on the matrix structure and volume fraction of TiC has been considered here. The charge calculations for composites T1, T2, T3, T4, and T5 were done by simple stoichiometric method aiming pure Fe, Fe-0.4% C, Fe-0.6% C, Fe-0.8% C, and Fe-1.0% C, respectively, as matrix and 13.5 vol% TiC (Table II). Both cast iron and graphite were used as the source of C for composites T1, T2, T3, T4 and T5. The amount of cast iron in the charge material for the synthesis of all the composites was kept constant. The amount of graphite was varied so as to achieve desirable matrix composition and volume fraction of TiC. However, it was recognized that carbon may get lost by oxidation during SHS reaction, and therefore 50 wt% excess of required stoichiometric amount of carbon was added in the charge material for the synthesis of all the composites. Excess carbon was added in the form of graphite. The amount of graphite, shown in Table II, is the required stoichiometric amount of graphite plus 50 wt% excess of required stoichiometric amount of total carbon (i.e., carbon from cast iron plus graphite, needed to get the desired matrix composition and volume fraction of TiC). Stoichiometric amount of aluminum, needed to reduce all the oxides, was added in the charge.

### 3.2. Melting procedure

The charge consisting of siliceous sand, Al powder, and C in the form of cast iron and graphite powder was thoroughly mixed and placed in a zircon painted clay-graphite crucible, which was kept inside a pit furnace to preheat the charge to a temperature of 775°C for half an hour. The crucible was removed from the furnace and then the reaction was triggered by adding magnesium turnings. The heat generated due to aluminothermic reaction was high enough to melt the charge completely and uniformly. A bottom pouring arrangement was made so that the liquid metal could be poured directly into a mould by opening the plug at the bottom of the crucible. A flow chart depicting the synthesis of Fe-TiC composite is shown in Fig. 1.

### 3.3. Chemical analysis

The chemical compositions of the as-cast composites, as determined by spectroscopic analysis, are given in Table III. All the composites contain a substantial amount of Al and Si. Silicon came from the reduction of $SiO_2$, present in the siliceous sand. Although a stoichiometric amount of Al was added, a part of Al remained unreacted due to the loss of $Fe_2O_3$, $SiO_2$ and $TiO_2$ into the slag and thus present in the composites.

TABLE III Chemical compositions of the as-cast composites

| Material | wt% Al | wt% Si | wt% Ti | wt% C | wt% Fe |
|---|---|---|---|---|---|
| T1 | 4.28 | 2.73 | 4.10 | 1.38 | Balance |
| T2 | 4.36 | 2.58 | 4.22 | 1.53 | Balance |
| T3 | 3.67 | 2.20 | 5.05 | 1.84 | Balance |
| T4 | 2.81 | 2.57 | 6.10 | 2.46 | Balance |
| T5 | 3.45 | 2.58 | 5.87 | 3.04 | Balance |

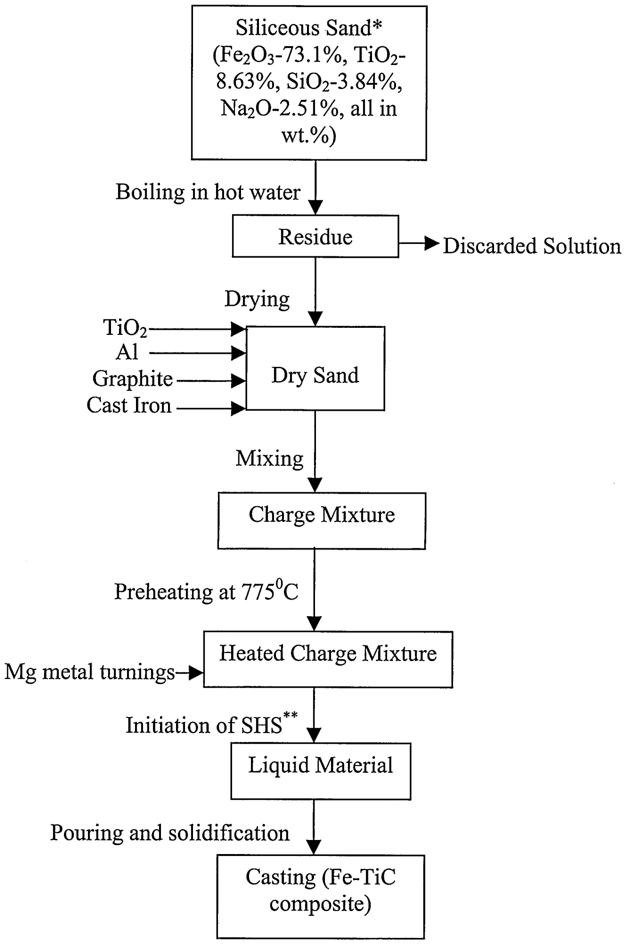

*Siliceous sand is a waste material from aluminum extraction plant.
**SHS means self-propagating high-temperature synthesis.

*Figure 1* Flow-sheet depicting the synthesis of Fe-TiC composite.

### 3.4. Metallography and X-ray diffraction (XRD) analysis

Metallographic samples of dimension 12 mm × 12 mm × 10 mm were cut from the middle portion of castings. The specimens were etched with 2% nital and they were examined using an optical microscope as well as a scanning electron microscope (SEM) equipped with an energy dispersive X-ray spectrometer (EDS). The various phases revealed by metallography were analyzed by the X-ray diffraction analyses in an X-ray diffractometer using the Co $K_\alpha$ radiation.

## 4. Results and discussion

The macrostructure of the cast ingot of the composites reveals that they are absolutely free from gas porosity and blow holes. This is due to the fact that aluminothermic reduction is a very high temperature synthesis reaction, which drives away the volatile impurities and absorbed gases from the molten product. The composites are also free from any slag inclusion. This is because of the fact that the heavier metallic phase and the lighter oxide phase get well separated by gravity, and the composite is cast by a bottom pouring arrangement. As a result, fully densified composites have been produced in the present investigation.

### 4.1. Microstructural characterization

The cast microstructures of composites T1 to T5 are shown in Fig. 2a to e. The micrographs clearly show that the reinforcing TiC particles are present in various types of matrices. The structures of the matrices in these materials vary from mostly ferritic type to ferrito-pearlitic type to almost completely pearlitic type. The matrix microstructure of T5 consists of pearlite plus cementite.

### 4.2. Microstructures of composites T1 to T4

The matrix of the composite T1 appears to be mostly ferritic type with the reinforcing TiC particles embedded in the matrix as shown in Fig. 2a. The reinforcing particles are TiC and they are identified by EDX (Fig. 3) and X-ray diffraction (Fig. 4) techniques. Some fine, bright colored phase is also observed in the structure. This phase is identified as $Fe_2Ti$ and forms because there is not enough C in the melt to react with Ti and therefore Ti concentration in the matrix reaches a high value leading to the formation of $Fe_2Ti$, as the solubility of Ti in ferrite decreases during cooling [15]. The formation of this phase is also evident from the ternary Fe-Ti-C phase diagram at the low C region [5]. The

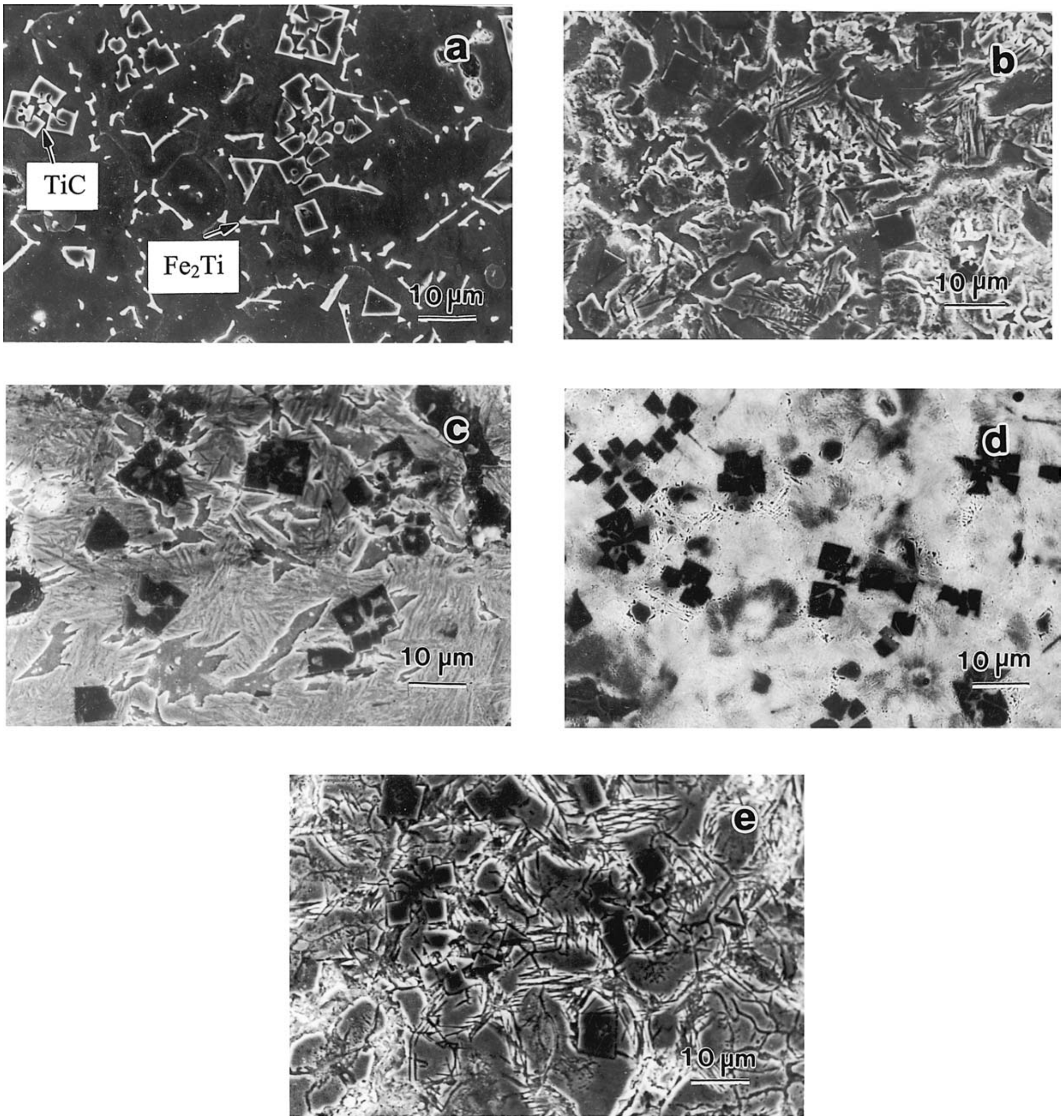

*Figure 2* SEM micrographs of composite: (a) T1 showing the distribution of TiC particles in ferritic type matrix, (b) T2 showing the distribution of TiC particles in ferrito-pearlitic type matrix, (c) T3 showing distribution of TiC particles in mostly pearlitic type matrix, (d) T4 showing distribution of TiC particles in fully pearlitic type matrix, and (e) T5 showing the distribution of TiC particles in pearlitic plus cementite type matrix.

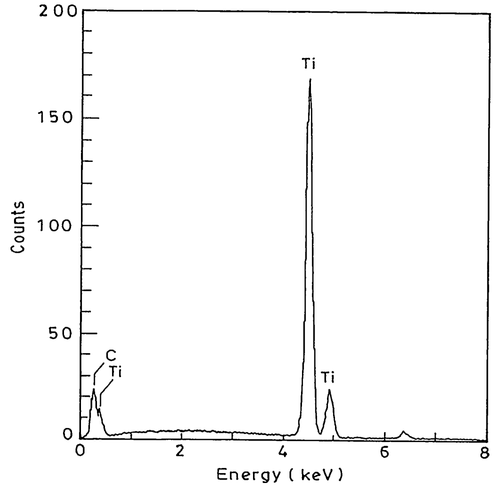

*Figure 3* EDX spectrum taken from a carbide particle (TiC).

X-ray data (Fig. 4) confirm the presence of the phases revealed in the microstructures. The volume fraction of TiC particles has been determined by a Leica image analyzer and is given in Table IV.

The microstructure of the as-cast material T2 is shown in Fig. 2b. The micrograph clearly shows that the reinforcing TiC particles are present in ferrito-pearlitic

TABLE IV Volume fractions of TiC in as-cast composites

| Material | Volume fraction of TiC (%) |
|---|---|
| T1 | 4.5 |
| T2 | 5.4 |
| T3 | 7.3 |
| T4 | 8.5 |
| T5 | 8.0 |

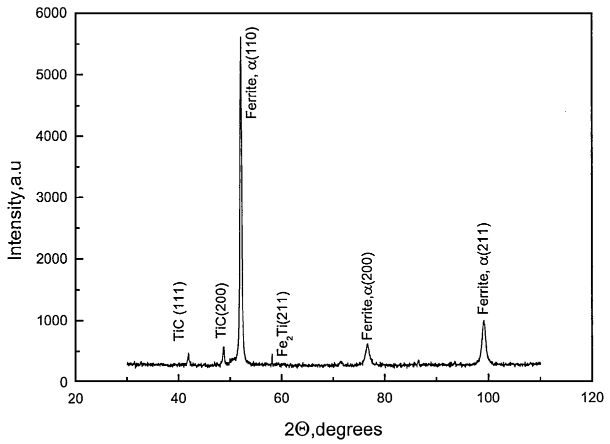

*Figure 4* X-ray diffraction pattern of as-cast T1 using Co $K_\alpha$ radiation.

type of matrix. This is clearly due to the effect of the C content of the matrix Fe. The matrix C content of plain carbon hypo-eutectoid steel can be determined by knowing the volume fraction of pearlite as 0.8 wt% C produces 100 percent of pearlite. The volume fraction of pearlite in composite T2 is measured by image analysis and it is found to be around 40%. Hence, approximate C content of the matrix is 0.32 wt%.

Microstructure of composite T3 is presented in Fig. 2c. The matrix of the material is mostly pearlitic type with pearlite volume fraction of about 75%. The approximate C content of the matrix is 0.6 wt%. The TiC particles are present mostly in cluster form.

Microstructure of composite T4 is presented in Fig. 2d. The matrix of the material T4 is essentially pearlitic type. The amount of pearlite type region is about 87% and this is simply because of the increase in C content of the charge mixture. Carbon availability in the melt dictates what type of steel matrix would form. Besides the increase in the pearlite content of the matrix, TiC volume fraction also increases from 4.5 vol% in T1 to 8.5 vol% in T4 even though the amount of $TiO_2$ in the charge remains same for all the composites (Table IV).

It is observed from Fig. 2a to d that TiC volume fraction as well as pearlite volume percent increase from composite T1 to T4. Increasing the C content of the charge mixture (in the form of graphite) from T1 to T4, TiC formation gets accelerated. Such fast formation of TiC in turn encourages the reduction of $TiO_2$ to elemental Ti ($3TiO_2$ (s) + 4Al (l) = Ti (l) + $2Al_2O_3$ (s)) because of the depletion of Ti in the molten Fe. As more amount of Ti is generated, the formation reaction of TiC is enhanced [17]. This explains the increase in volume fraction of TiC particles in the composites with the increase in C content of the charge mixture. It has been also found that with an increase in C content of the charge the pearlite volume fraction increases, as the C content of the matrix Fe also increases.

## 4.3. Microstructure of composite T5

The micrograph of composite T5 shows pearlitic type matrix along with some amount of $Fe_3C$ (Fig. 2e). The presence of $Fe_3C$ in the structure apparently suggests that the Fe matrix formed in this material is like hypereutectoid steel. But the morphology of the $Fe_3C$ phase is not exactly similar to the carbide network usually present in the hypereutectoid steel structures. It is suggested by Raghunath *et al.* that in the presence of both Fe and Ti, C reacts preferentially with Ti to form TiC [8]. Titanium depletion occurs in the melt due to the formation of TiC resulting in the increase of the activity of Fe, which in turn may lead to the formation of $Fe_3C$. Therefore, one may conclude that there exists a critical level of C concentration below which only TiC forms in the Fe-Ti-C system, whereas above the critical level of C concentration both TiC and $Fe_3C$ may be found in the microstructure.

## 4.4. Mechanism of formation of matrix and reinforcement

Titanium carbide-reinforced Fe-based composites have been synthesized in a single stage by aluminothermic reduction of siliceous sand in the presence of C. Important reactions leading to the formation of Fe-TiC composite can be written as

$$Fe_2O_3\,(s) + 2Al\,(l) = 2Fe\,(l) + Al_2O_3\,(s) \qquad (1)$$

$$3TiO_2\,(s) + 4Al\,(l) + 3C\,(s) = 3TiC\,(s) + 2Al_2O_3\,(s) \qquad (2)$$

Along with reactions (1) and (2) other reactions are also taking place such as:

$$3SiO_2\,(s) + 4Al\,(l) = 3Si\,(l) + 2Al_2O_3\,(s) \qquad (3)$$

$$Fe\,(l) + Si\,(l) + Al\,(l) + C\,(s) = \text{Fe-Al-Si-C}\,(l) \qquad (4)$$

Fe, Ti, and Si get reduced from the respective oxides. Iron, thus generated, forms the matrix along with C, Al and Si. Matrix also contains a substantial amount of Al. This is inevitable because of the presence of Al in the system as the main reducing agent. A part of the unreacted Al remains in solution in Fe and joins the matrix phase. Titanium reacts with the C to form the TiC particles. Thus, the reinforcing component in the composites is generated *in-situ*. The morphology of the carbide particles is interesting to note. They are present both as single and as combination of particles forming clusters (Fig. 5). It is quite likely that a supersaturated solution

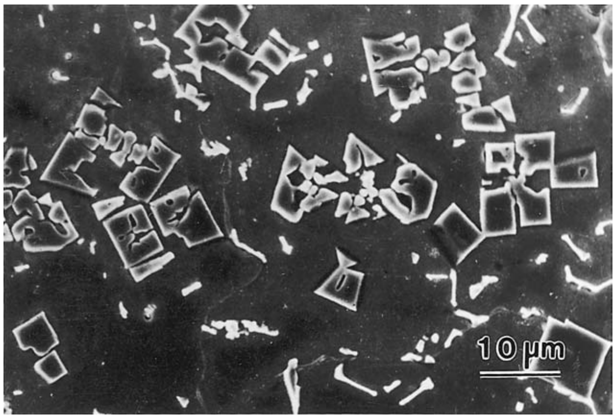

*Figure 5* SEM micrograph of as-cast composite T1 showing clustering of TiC particles.

of Ti and C in Fe forms with simultaneous formation of TiC through the reaction of Ti (l) and carbon (s) as C is added in the form of cast iron plus graphite. Freshly reduced Ti from $TiO_2$ instantly reacts with graphite to form TiC and also simultaneously a solution of Fe-Ti-C is formed. Hence, TiC particles in this system may be considered to form according to reactions (5) and (6) by combination mechanism of solid-liquid reaction and solution-precipitation like that of Al-Ti-C system [18].

$$\underline{\mathrm{Ti}} + \mathrm{C\ (s)} = \mathrm{TiC\ (s)} \qquad (5)$$

$$\underline{\mathrm{Ti}} + \underline{\mathrm{C}} = \mathrm{TiC\ (s)} \qquad (6)$$

where, $\underline{\mathrm{Ti}}$ and $\underline{\mathrm{C}}$ mean Ti and C in solution.

During cooling, the solubility of both Ti and C decreases. Therefore, excess amounts of Ti and C get precipitated as fresh TiC particles in the matrix and as well as on the pre-existing TiC particles, as formed according to reaction 5. Formation of cluster of TiC is due to the precipitation of TiC particles on the existing ones. This is justified by the minimization of nucleation energy. The clustering of TiC particles may be misinterpreted as inhomogeneity in the local scale, however microstructure is uniform all throughout the casting.

## 4.5. Effect of heat treatment on as-cast microstructures

### *4.5.1. Annealing*

The hardness of TiC particles in the as-cast composites has been found to vary between 1800–2200 HV. The hardness of stoichiometric TiC particles is 3200 HV [19]. The microhardness measurement of TiC particles in the as-cast composites indicates that TiC particles are nonstoichiometric in nature in the as-cast composites. The kinetics of thermit reaction is very first. Aluminum reduces titanium dioxide and reduced Ti reacts with available carbon to form TiC. TiC also precipitates from supersaturated solution of Fe-Ti-C. Due to

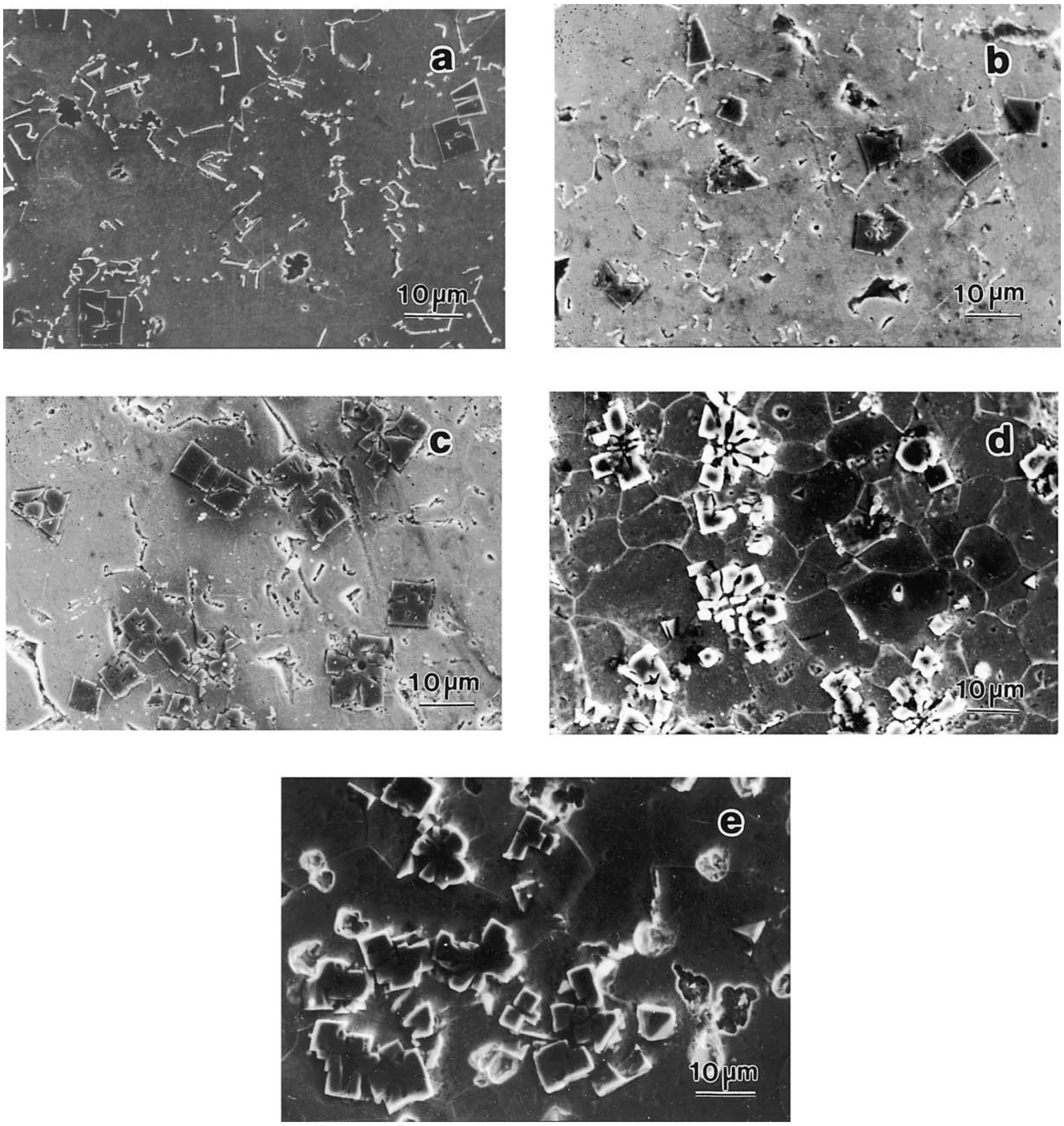

*Figure 6* SEM micrographs of composite: (a) T1, (b) T2, (c) T3, (d) T4, and (e) T5, annealed at 900°C for 6 h.

very first kinetics of thermit reaction and high cooling rate during solidification (metal mould was used for casting), there is very little time for reaction as well as diffusion. Hence, TiC does not get sufficient time to attain stoichiometry.

It is reported that the extent of nonstoichiometry of TiC decreases by the rejection of Ti from the carbide or by carbon pick-up from the matrix [20–22]. In order to assess the microstructural stabilities of the as-cast composites, they were subjected to annealing at 900°C for different times (1, 3, and 6 h). Fig. 6a shows the SEM micrograph of composite T1, annealed at 900°C for 6 h. The micrograph consists of ferritic type matrix, TiC particles and a second phase. The volume fraction of TiC is lower in the heat-treated sample compared to the as-cast one. This is owing to the dissolution of TiC. Since the matrix of T1 contains a low amount of C, it is the Ti, which diffuses out of TiC into the matrix during annealing. As a result, a second phase consisting of Fe and Ti, i.e., $Fe_2Ti$ forms and hence the volume fraction of $Fe_2Ti$ increases from as-cast to annealed composite. Microstructural evidence confirms that Ti diffuses out of TiC particles to lower the extent of nonstoichiometry.

Fig. 6b shows the SEM micrograph of composite T2, annealed at 900°C for 6 h. The micrograph consists of ferritic type matrix, TiC particles and a second phase consisting of Fe and Ti. The second phase $Fe_2Ti$ forms as a result of diffusion of Ti from TiC to the matrix. The matrix of composite T2 in the as-cast condition is ferrito-pearlitic type and transforms to ferritic type after annealing. This indicates that initially C diffuses from the matrix to TiC to decrease the extent of nonstoichiometry of TiC, resulting the transformation of matrix from ferrito-pearlitic type to ferritic type. However, after a while Ti diffuses out of TiC to decrease the extent of nonstoichiometry (as the C content in the matrix decreases to a very low value) resulting in the formation of the $Fe_2Ti$ phase as in composite T1.

Fig. 6c shows the SEM micrograph of composite T3, annealed at 900°C for 6 h. The micrograph of the composite consists of ferritic type matrix and TiC particles. No second phase is noticed in the micrograph. These observations indicate that after annealing, mostly pearlitic type matrix in the as-cast condition is converted into ferritic type. This is due to the diffusion of C from the matrix to TiC particles so that the extent of nonstoichiometry of TiC decreases.

Fig. 6d shows the SEM micrograph of composite T4, annealed at 900°C for 6 h. The micrograph consists of ferritic type matrix and TiC particles. Here, C from the matrix diffuses into nonstoichiometric TiC to reduce the extent of nonstoichiometry resulting in the transformation of matrix from pearlitic type to ferritic type.

Fig. 6e shows the SEM micrograph of composite T5, annealed at 900°C for 6 h. The micrograph consists of ferritic type matrix along with the dispersion of TiC particles. The C content of the matrix is high in the composite T5 since it is hyper-eutectoid type. It is quite expected that C from matrix difuses into nonstoichiometric TiC particles and matrix of composite T5 changes from pearlitic plus cementite type in the as-cast state to ferritic type in the annealed condition.

Dissolution as well as microstructural modification occurs in composite T1, whereas only structural

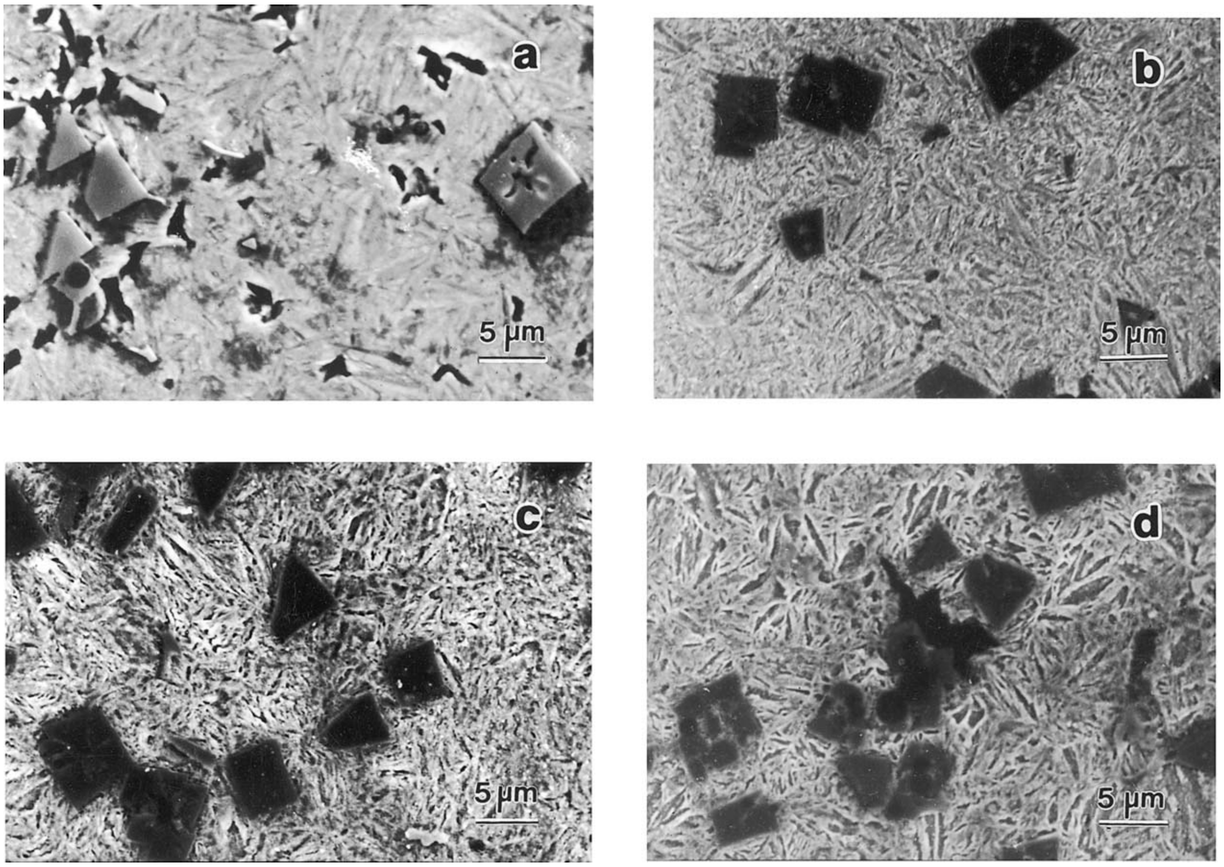

*Figure 7* SEM micrographs of composite T4: (a) as-quenched, (b) tempered at 200°C, (c) tempered at 400°C and (d) tempered at 500°C.

modification occurs in composites T2, T3, T4 and T5 during annealing. This is not desirable as the hardness of all the composites fall drastically after annealing (discussed in part—II of the paper).

### *4.5.2. Quenching and tempering*

To study the effect of quenching treatment on the microstructure and abrasive wear resistance property, material T4 was quenched from 900°C in brine solution. The SEM micrograph of the as-quenched T4 composite is shown in Fig. 7a. It clearly indicates the formation of martensite as the matrix. Interestingly, no dissolution of TiC particles is observed. This can be attributed to high C content of the matrix of composite T4. As-quenched material is tempered at 200, 400, and 500°C for half an hour. The microstructures of the samples tempered at 200, 400, and 500°C are shown in Fig. 7b, c, and d, respectively. No significant microstructural change occurs when tempered at 200°C. Needle like cementite forms and coarsens during tempering at 400 and 500°C.

## 5. Conclusions

1. It is possible to synthesize TiC reinforced Fe-based composite by a simple aluminothermic reduction of siliceous sand in the presence of carbon, and therefore a waste is converted into a value added product by a cost-effective process.

2. Variation of amount of carbon as graphite in the charge mixture leads to several types of matrix structures ranging from almost fully ferritic type to fully pearlitic type and then to pearlitic plus cementite type.

3. The TiC particles in the as-cast composites are nonstoichiometric in nature and it lowers its extent of nonstoichiometry by the rejection of Ti from the carbide or by carbon pick-up from the matrix during annealing. In the csae of mostly ferritic type matrix, Ti diffuses out of TiC particles to lower the extent of stoichiometry resulting in a lower volume fraction of TiC together with the formation of $Fe_2Ti$ phase. However, in the case of mostly pearlitic type or pearlitic plus cementite type matrix TiC decreases its extent of nonstoichiometry by taking carbon from the matrix resulting in the transformation of matrix from pearlitic type or pearlitic plus cementite type to ferritic type.

## Acknowledgment

The authors wish to acknowledge The Department of Science and Technology, The Government of India, for the financial help received to carry out this research work.

## References

1. E. PAGOUNIS, M. TALVITIE and V. K. LINDROOS, *Metall. Mater. Trans.* A **27A** (1996) 4171.
2. *Idem., Powder Metall.* **40** (1997) 55.
3. *Idem., Metall. Mater. Trans.* A **27A** (1996) 4183.
4. J. D. BOLTON and A. J. GANT, *Powder Metall.* **40** (1997) 143.
5. T. Z. KATTAMIS and T. SUGANUMA, *Mater Sci. Engng.* A **A128** (1990) 241.
6. B. S. TERRY and O. S. CHINYMAKOBVU, *J. Mater. Sci. Lett.* **10** (1991) 628.
7. *Idem., Mater. Sci. Technol.* **8** (1992) 399.
8. C. RAGHUNATH, M. S. BHAT and P. K. ROHATGI, *Scripta Metall.* **32** (1995) 577.
9. S. SKOLIANOS, T. Z. KATTAMIS, M. CHEN and B. V. CHAMBERS, *Mater. Sci. Engng.* A **183** (1994) 195.
10. B. S. TERRY and O. S. CHINYMAKOBVU, *Mater. Sci. Technol.* **7** (1991) 842.
11. R. K. GALGALI, Ph.D thesis, Indian Institute of Technology, Kharagpur, 1995.
12. Y. CHEN, *Scripta Materialia.* **36** (1997) 989.
13. L. L. WANG, Z. A. MUNIR and Y. M. MAXIMOV, *J. Mater. Sci.* **28** (1993) 3693.
14. T. K. BANDYOPADHYAY and K. DAS (unpublished research).
15. T. B. MASSALSKI, "Binary Alloy Phase Diagram" (ASM International, Materials Park, OH, 2001) p. 1785.
16. Y. M. LAKHTIN, "Engineering Physical Metallurgy and Heat-Treatment" (Mir Publishers, Moscow, 1990) p. 150.
17. A. A. POPOV and M. M. GASIK, *Scripta Materialia* **35** (1996) 629.
18. S. C. TJONG and Z. Y. MA, *Mater. Sci. Engng.* **29** (2000) 49.
19. I. E. CAMPBELL and E. M. SHERWOOD, "High Temperature Materials and Technology" (John Wiley and Sons Inc., USA, 1967) p. 324.
20. N. FRAGE, L. LEVIN, E. MANOR, R. SHNECK and J. ZABICKY, *Scripta Materialia* **35** (1996) 798.
21. *Idem., ibid.* **35** (1998) 791.
22. N. FRAGE, *Metall. Mater. Trans* B **30B** (1999) 857.

*Received 4 August 2003*
*and accepted 2 April 2004*